ISCI, Volume *11*

Supplemental Information

Ternary Heterostructural Pt/CN_x/Ni as a Supercatalyst for Oxygen Reduction

Teng Chen, Yida Xu, Siqi Guo, Dali Wei, Luming Peng, Xuefeng Guo, Nianhua Xue, Yan Zhu, Zhaoxu Chen, Bin Zhao, and Weiping Ding

Supplemental Information

Supplemental Data Items

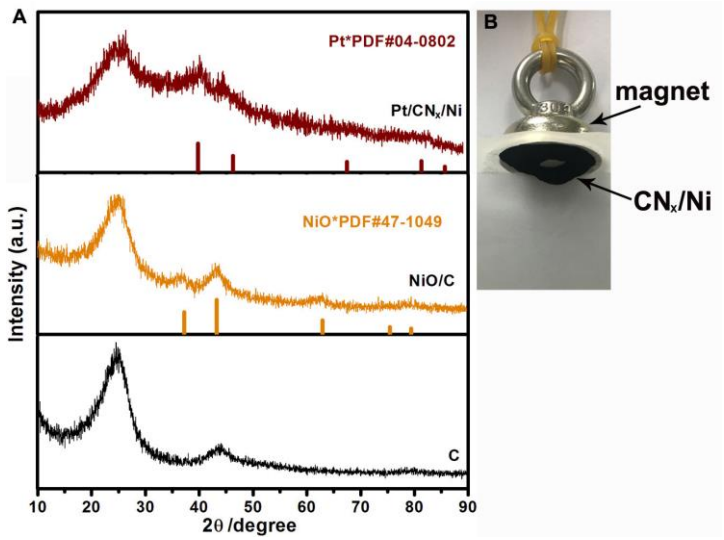

Figure S1. Characterization of as-prepared Pt/CN_x/Ni and the intermediates in its preparation process, related to Figure 2. (A) XRD patterns for Pt/CN_x/Ni and the intermediates in its preparation process, (B) a picture of adsorbed CN_x/Ni on magnet to reveal the magnetism of CN_x/Ni.

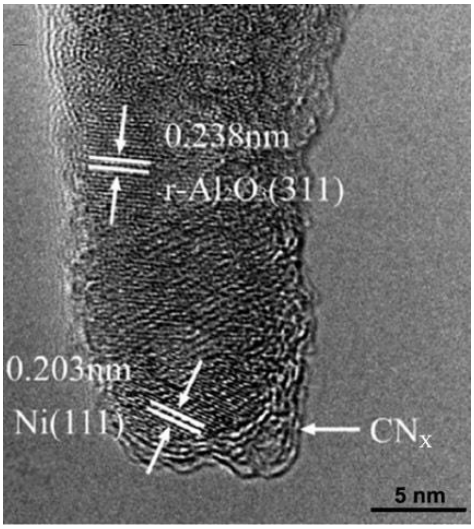

Figure S2. Characterization of CN_x/Ni/Al_2O_3, related to Figure 2. HRTEM images of CN_x/Ni/Al_2O_3. The thickness of CN_x is approximately 1.5 nm.

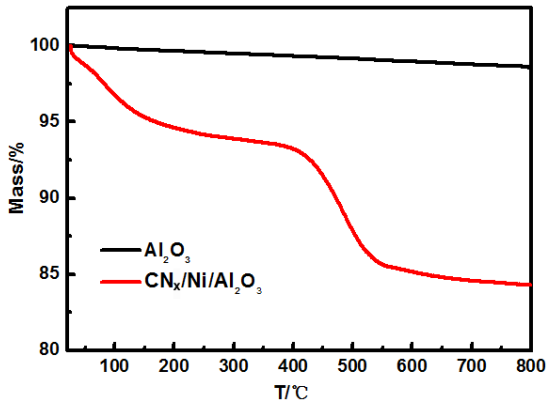

Figure S3. Characterization of Al_2O_3 and $CN_x/Ni/Al_2O_3$, related to Figure 2. Thermogravimetric profiles for Al_2O_3 and $CN_x/Ni/Al_2O_3$.

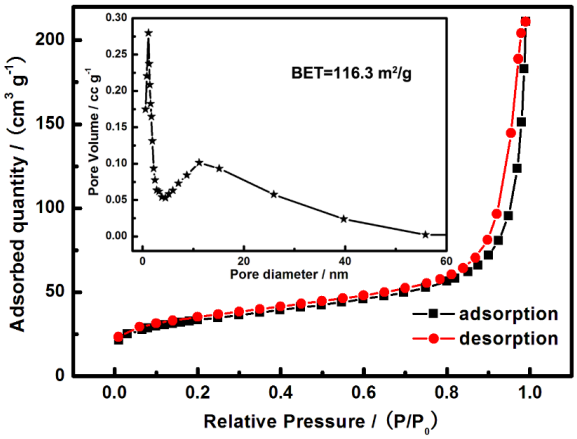

Figure S4. Characterization of NiO/C, related to Figure 2. N_2 adsorption/desorption isotherms and pore size distributions of NiO/C.

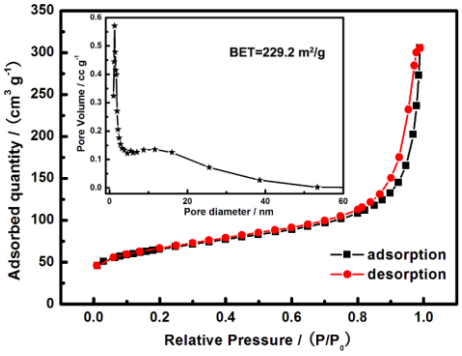

Figure S5. Characterization of XC-72R support, related to Figure 2. N_2 adsorption/desorption isotherms and pore size distributions of C.

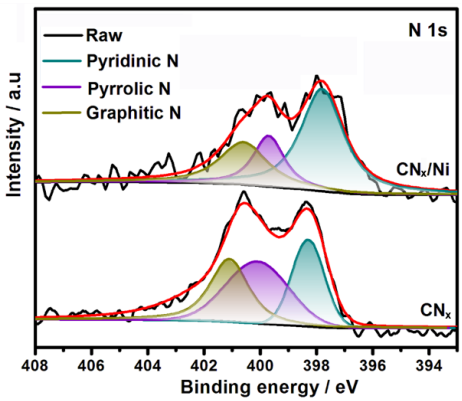

Figure S6. Electronic equilibration across the CN_x/Ni interface, related to Figure 3. Deconvoluted spectra of nitrogen 1s of CN_x/Ni and CN_x.

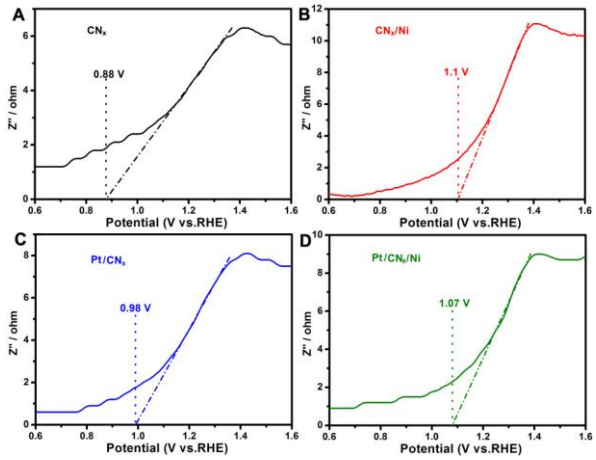

Figure S7. The electrochemical study of CN_x, CN_x/Ni, Pt/CN_x and Pt/CN_x/Ni, related to Figure 3. Impedance-potential curves of (A) CN_x, (B) CN_x/Ni, (C) Pt/CN_x and (D) Pt/CN_x/Ni for determining the flat-band potentials of samples.

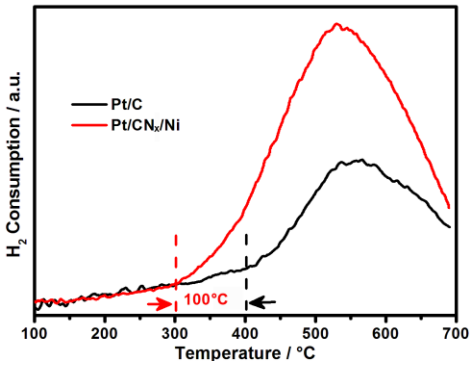

Figure S8. Characterization of Pt/C and Pt/CN_x/Ni, related to Figure 5. Redox O_2-H_2 titration curves for Pt/C and Pt/CN_x/Ni.

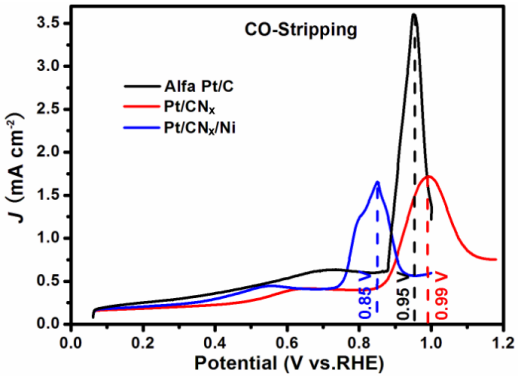

Figure S9. The electrochemical study of Pt/C, Pt/CN$_x$ and Pt/CN$_x$/Ni, related to Figure 5.
CO-Stripping curves of Alfa Pt/C, Pt/CN$_x$ and Pt/CN$_x$/Ni for probing the adsorption properties of the Pt catalysts.

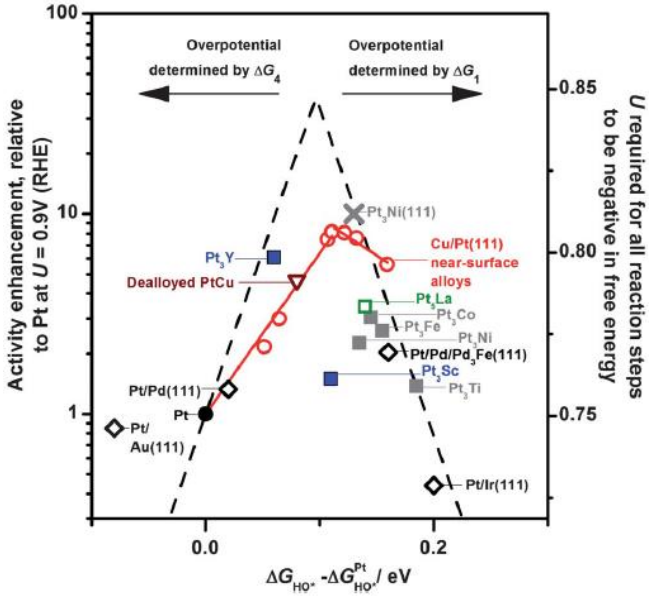

Figure S10. The rate-determining step in the volcano type activity plots, related to Figure 5. Volcano plot for different catalysts with Pt-overlayers: experimental ORR activity enhancement as a function of hydroxyl binding energy, ΔG_{HO}*, both relative to pure Pt. All data are at U = 0.9 V, with respect to a reversible hydrogen electrode (RHE) (Stephens et al., 2012).

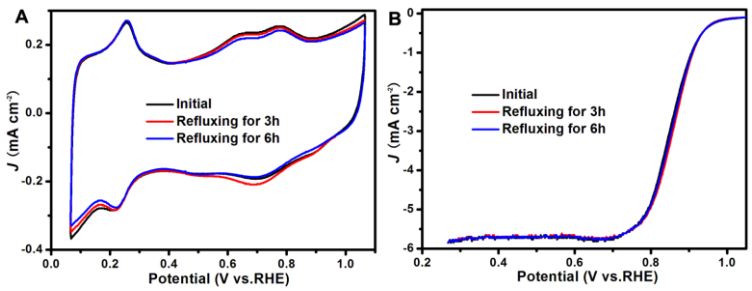

Figure S11. The electrochemical study of Pt/CN$_x$/Ni electrode, related to Figure 5. (A), CV curves and (B), ORR polarization curves of Pt/CN$_x$/Ni catalyst before and after refluxing in 1 M H_2SO_4 at 353 K in alkaline solution (0.1 M KOH). The scan rate is 20 mV s^{-1}.

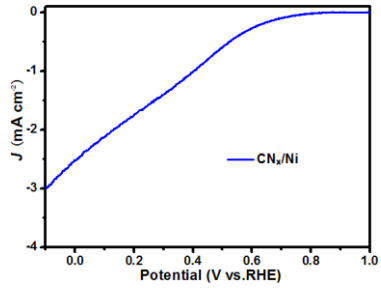

Figure S12. The electrochemical study of Pt/CN_x/Ni electrode, related to Figure 5. ORR polarization curves of CN_x/Ni in 0.1M $HClO_4$ aqueous solution at a sweep rate of 20 mV s^{-1}.

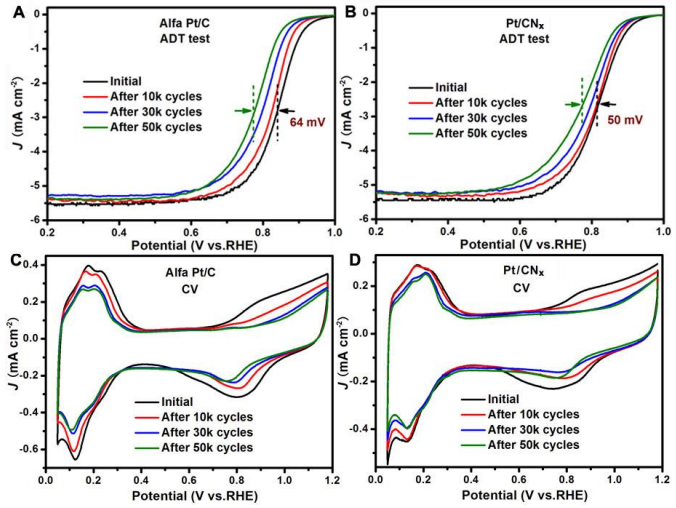

Figure S13. The stability study of Pt/C and Pt/CN_x electrodes, related to Figure 5. ORR polarization curves of Alfa Pt/C (A) and Pt/CN_x (B), CV curves of Alfa Pt/C (C) and Pt/CN_x (D) before and after 50000 CV cycles between 0.6 and 1.0 V versus RHE. The sweep rate for the accelerated deterioration test (ADT) is 200 mV s^{-1}. All the curves were recorded at 298 K in 0.1M $HClO_4$ aqueous solution at a sweep rate of 20 mV s^{-1}.

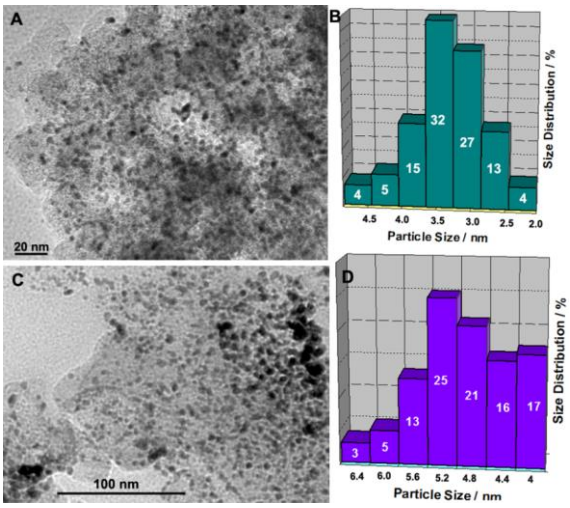

Figure S14. Characterization of Pt/C, related to Figure 5. TEM images of commercial Pt/C (Alfa) before (A) and after (C) ADT test, and their corresponding size distribution histogram by statistical analysis of 300 Pt NPs (B and D).

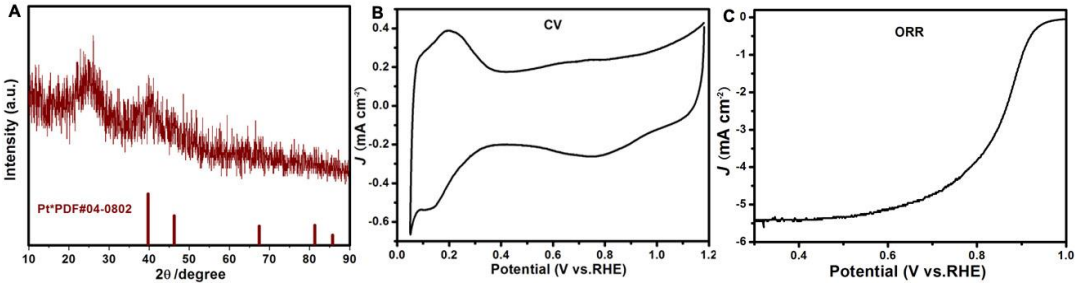

Figure S15. Characterization of Pt/CN$_x$/Co, related to Figure 5. (A) XRD patterns for Pt/CN$_x$/Co. (B) CV and (C) ORR curves of Pt/CN$_x$/Co catalyst.

Table S1. The element content and geometric analysis for the series of Pt/CN$_x$/TM samples, related to Figure 5.

	Pt/CN$_x$	Pt/CN$_x$/Ni	Pt/CN$_x$/Co	Pt/C (Alfa)
Element content Determined by XRF (wt.%)	Pt: 6.0%	Pt: 6.2%, Ni: 5.6%	Pt: 6.5%, Co: 4.8%	Pt: 20%
Specific ECSA (m^2/g_{Pt})	Initial: 125.5 CV-10 k: 115.6 CV-30 k: 94.2 CV-50 k: 91.5	Initial: 122.0 CV-10 k: 125.9 CV-30 k: 110.2 CV-50 k: 109.4	Initial: 121.6	Initial: 77.2 CV-10 k: 64.2 CV-30 k: 50.3 CV-50 k: 46.4

Transparent Methods

Materials Synthesis

Nano carbon support (Vulcan XC-72R). A desired amount of commercial Vulcan XC-72R was dispersed in acetone, stirred for 3 h at room temperature, filtered and dried in a vacuum oven at 343 K for 4 hours. Then, dispersing the resulted carbon powder in an aqueous solution of 10% nitric acid and 30% hydrogen peroxide (V_{HNO3} : V_{H2O2} = 2:1) and stirring at 333 K for 5 hours with reflux. The carbon support was obtained after suction filtering, water washing to neutral, drying in a vacuum oven at 353 K.

Preparation of NiO/C. The NiO/C powder was prepared by an incipient-wetness impregnation method. Briefly, 200 mg carbon support was mixed with moderate amounts of nickel nitrate solution with desired concentration, stirred and agitated by ultrasonic for 20 min. The obtained powder was dried at 353 K overnight and calcined at 573 K for 1 h in argon.

Preparation of CN_x/Ni support. The composite with Ni NPs capped by CN_x layer (CN_x/Ni) was prepared by encapsulating polymer of ethylenediamine and carbon tetrachloride on NiO/C and carbonizing in inert atmosphere according to our previous work (Fu et al., 2014). Specifically, 100 mg NiO/C powder was dispersed in 15 mL *m*-xylene by ultrasonic. 250 mg ethylenediamine and 500 mg carbon tetrachloride were dropwise added into the above suspension sequentially. Then, the suspension was stayed at 363 K for 4 h and 413 K for another 4 h, respectively. After cooling to room temperature, the polymer-coated NiO/C powder was washed with *m*-xylene and dried at 393 K overnight. The CN_x/Ni/C support, abbreviated as CN_x/Ni in the context, was obtained after carbonizing at 873 K for 6 h and 1173 K for 30 min in flowing N_2. The NiO was reduced to metallic Ni in the reducing atmosphere during the treatment at high temperatures.

Preparation of Pt/CN_x/Ni catalyst. In order to avoid the formation of Ni-Pt alloy, the CN_x/Ni support was refluxing in 1 M H_2SO_4 at 353 K for 4 h before loading Pt NPs. Because of the high graphitization, the CN_x shell is hydrophobic and cannot offer sites to anchor metal nanoparticles. To solve the problem, the CN_x shell was coated by a little amount of polydopamine with the following steps. 50 mg of CN_x/Ni powder was dispersed in 1mg/mL dopamine solution, which was prepared by dissolving dopamine hydrochloride in 10 mM tris buffer solution (pH 8.5). After stirring in air for 30 min, the surface-modified CN_x/Ni support was obtained by centrifugation and dehydration. The deposition of Pt NPs on CN_x/Ni support was operated by an incipient-wetness impregnation method. That is, transferring the as-obtained surface-modified CN_x/Ni into moderate amounts of chloroplatinic acid solution with desired concentration, dispersing and agitating by ultrasonic for 40 min and staying at room temperature overnight. After drying at 343 K, the chloroplatinic acid was reduced at 673 K for 3 h in 5.05 vol.% H_2/N_2 mixed gas with a heating rate of 2 °C/min.

Preparation of Pt/CN_x/Co catalyst. The Pt/CN_x/Co catalyst was prepared using a same procedure with Pt/CN_x/Ni, just substituting the nickel nitrate solution with cobalt nitrate solution in the preparation of CoO/C.

Characterization. X-ray diffraction (XRD) patterns were collected on a Phillips X'pert Pro diffractometer with Co Kα radiation at 40 kV and 35 mA. Field Emission High Resolution TEM and Energy-dispersive X-ray spectroscopy (EDX) were collected on Tecnai G2 F30 S-Twin TEM with an accelerating voltage of 300 kV. The X-ray photoelectron spectroscopy (XPS) tests were performed on a PHI 5000 Versa Probe equipped with a hemispherical electron analyzer and monochromatic Al Kα X-ray exciting source. Thermogravimetric (TG)

curves were collected on a STA 449C-Thermal Star 300 instrument (Netzsch, Germany) in air atmosphere with a heating rate of 10 $K \cdot min^{-1}$ to 1073 K. Redox of O_2-H_2 titration profiles were recorded on a thermal conductivity detector with the following procedure. 0.1 g sample was pretreated in 5.05 vol. % H_2/N_2 flow at 300 °C for 1 h and cooled to 30°C and then switched to oxygen. After putting the sample in O_2 flow at 30 °C for 1 h, switching O_2 to 5.05 vol. % H_2/N_2 flow to purge the adsorbed O_2 physically. Finally, raising the temperature from 30 to 700 °C at a rate of 10 °C min^{-1} under 5.05 vol. % H_2/N_2 flow and measuring the reduction curve.
s (229.2 m^2/g) and *n* are the surface area of C and the number of Ni nanoparticles on 1g C.

The number of layers (*n*) of wrapped CN_X:

$$n = \frac{m}{\rho \cdot s \cdot d} \quad \text{(S1)}$$

m and ρ (2.25 g/cm^3) (Ci et al., 2007) are the quality and density of CN_X, *s* (116.3 m^2/g) is the superficial area of NiO/C, *d* (0.32-0.5 nm) (Lee et al., 2008; Zhao et al., 2014; Jiang et al., 2016) is the thickness of monolayer CN_X.

The distance of adjacent Ni nanoparticles:

$$d_{Ni} = 2(s/n\pi)^{1/2} \quad \text{(S2)}$$

The specific surface area of the Pt NPs:

$$s = 4\pi r^2 * 1 / (\rho * 4/3\pi r^3) \quad \text{(S3)}$$

ρ (21.45 g/cm^3) is the density of Pt.

Electrochemical experiment. The electrochemical tests were performed on an electrochemical workstation (CHI 730D) using a three-electrode system. The catalyst ink was prepared by dispersing the obtained powder (5 mg) in isopropanol (970 μL) and 5 wt. % Nafion (30 μL) mixed solution by ultrasonic dispersion. Subsequently, 5 μL of the ink was transferred onto a glassy carbon electrode (φ = 5.6 mm, 0.246 cm^{-2}) and dried at room temperature. Pt wire and Ag/AgCl electrode were used as the counter and reference electrodes in 0.1 M $HClO_4$ solution, respectively.

Cyclic voltammetry (CV) was conducted at the potential of 0.05-1.2 V (*vs*. RHE) with a scan rate of 5 mV s^{-1} in N_2-saturated electrolyte.

CO-stripping voltammetry was conducted at the potential of 0.06-1.0 V (*vs*. RHE) with a scan rate of 50 mV s^{-1}. Prior to this, the working electrode was inserted into N_2-saturated electrolyte and held at the potential of 0.06 V (*vs*. RHE) for 15 min to electrochemically clean the catalyst surface. Then, CO was bubbled into the electrolyte while holding the potential at 0.06 V (vs. RHE) to poison the electrode surface. Afterwards, N_2 was bubbled into the electrolyte to remove the residual CO.

RDE system was used to study the ORR activity in O_2-saturated electrolyte at the potential of 0.05-1.2 V (*vs.* RHE) with a scan rate of 20 mV s^{-1} and rotation rate of 1600 rpm at 298 K. All the ORR curves were iR corrected. The accelerated deterioration tests (ADTs) was completed by applying the cyclic voltammetry between 0.6 and 1.0 V (*vs.* RHE) with a sweep rate of 200 mV/s for 50,000 cycles in O_2-saturated electrolyte.

The conduction band (CB) level of the samples were determined from the linear potential plots based on the Mott-Schottky equation. The linear potential plots were measured by electrochemical impedance spectroscopy (EIS) using a conventional three-electrode system, in which the Pt wire and Ag/AgCl electrode were used as the counter and reference electrode, respectively. The working electrode was prepared by dripping catalyst ink on a glassy carbon electrode (φ = 0.5 mm) and drying at room temperature. The measurements were performed in darkness at a scan rate of 25 mV/s and a frequency of 1 kHz.

Supplementary References

Ci, L., Vajtai, R. and Ajayan, P. M. (2007) Vertically aligned large-diameter double-walled carbon nanotube arrays having ultralow density. J. Phys. Chem. C *111*, 9077-9080.

Fu, T., Wang, M., Cai, W., Cui, Y., Gao, F., Peng, L., Chen, W., and Ding, W. (2014). Acid-resistant catalysis without use of noble metals: carbon nitride with underlying nickel. ACS Catal. *4*, 2536-2543.

Jiang, W., Luo, W., Zong, R., Yao, W., Li, Z., and Zhu, Y. (2016) Polyaniline/Carbon Nitride Nanosheets Composite Hydrogel: A Separation-Free and High-Efficient Photocatalyst with 3D Hierarchical Structure. Small *12*, 4370-4378.

Lee, C., Wei, X., Kysar, J. W. and Hone, J. (2008) Measurement of the elastic properties and intrinsic strength of monolayer graphene. Science *321*, 385-388.

Stephens, I., Bondarenko, A., Grønbjerg, U., Rossmeisl, J. and Chorkendorff, I. (2012). Understanding the electrocatalysis of oxygen reduction on platinum and its alloys. Energy Environ. Sci. *5*, 6744-6762.

Zhao, Y., Li, X., Du, Y., Chen, G., Qu, Y., Jiang, J., and Zhu, Y. (2014) Strong light-matter interactions in sub-nanometer gaps defined by monolayer graphene: toward highly sensitive SERS substrates. Nanoscale *6*, 11112-11120.